

# Comparison of Dynamical Heterogeneity in Hard-Sphere and Attractive Glass Formers

David R. Reichman

*Department of Chemistry and Chemical Biology, Harvard University, Cambridge, MA 02138*

Eran Rabani

*School of Chemistry, Tel Aviv University, Tel Aviv 69978, Israel*

Phillip L. Geissler

*Department of Chemistry, University of California,  
and Physical Biosciences and Materials Sciences Divisions,  
Lawrence Berkeley National Laboratory, Berkeley, CA 94720*

(Dated: February 8, 2020)

Using molecular dynamics simulations, we have determined that the nature of dynamical heterogeneity in jammed liquids is very sensitive to short-ranged attractions. Weakly attractive systems differ little from dense hard-sphere and Lennard-Jones fluids: Particle motion is punctuated and tends to proceed in steps of roughly a single particle diameter. Both of these basic features change in the presence of appreciable attractions. Transient periods of particle mobility and immobility cannot be discerned at intermediate attraction strength, for which structural relaxation is greatly enhanced. Strong attractions, known to dramatically inhibit relaxation, restore bimodality of particle motion. But in this regime, transiently mobile particles move in steps that are significantly more biased toward large displacements than in the case of weak attractions. We discuss these results in the context of spatial patterns of facilitating defects.

Dynamical heterogeneity is perhaps the most revealing feature of relaxation in deeply supercooled liquids. A high-temperature fluid is dynamically homogeneous in the sense that the local environment restricting fluctuations of any given particle is, for all important purposes, identical to that surrounding any other particle, even on the short time scales of basic microscopic motions. The distribution  $P(\delta\mathbf{r}, t)$  of particle displacements  $\delta\mathbf{r}$  as a function of time  $t$  provides a quantitative measure of such uniformity. Results of molecular dynamics simulations indicate that  $P(\delta\mathbf{r}, t)$  is Gaussian over a wide range of displacements, as would be expected from a mean-field perspective, for typical dense fluids<sup>1</sup>. The microscopic environments constraining particle motion in a glassy material are by contrast profoundly nonuniform, even on the long time scales of large-wavelength relaxation<sup>2,3,4,5</sup>. This fact has been clearly demonstrated by experiments that focus on dynamics of single probe molecules<sup>6</sup> or subsets of molecules in a pure liquid that relax more slowly than the average<sup>7,8</sup>. As a result,  $P(\delta\mathbf{r}, t)$  develops substantial weight in the wings, reflected in appreciably nonzero values of the non-Gaussian parameter  $\alpha_2(t) = \frac{3}{5} \langle \delta r^4(t) \rangle / \langle \delta r^2(t) \rangle^2 - 1$ . Microscopy studies of colloidal suspensions have confirmed this expectation<sup>9</sup>.

Through extensive computer simulations, a detailed picture of dynamical heterogeneity in simple jammed liquids (e.g., a binary mixture of Lennard-Jones spheres) has developed<sup>10</sup>. At low temperatures, the majority of particles are confined within cages, composed of neighboring particles, that may persist for very long times. Eventually, a rare, collective rearrangement frees a particle from its cage, transiently allowing it to move rapidly over distances comparable to a particle diameter. Since

such a displacement itself facilitates local rearrangement, transient mobility appears to propagate continuously and with some degree of directionality. Schematic models of glassiness have been constructed with only these features in mind<sup>11,12,13</sup>. They account for a surprising variety of anomalous behaviors and yield unique scaling predictions for the length and time scales characterizing relaxation<sup>13,14,15</sup>.

These basic features of dynamical heterogeneity have little to do with the identity of particles comprising a glassy material or with the interactions between them. They have been reported for many model atomic liquids as well as for viscous silica, a network-forming liquid which vitrifies with qualitatively different temperature dependence<sup>16</sup>. It is therefore tempting to presume that the scenario sketched above is universal among supercooled molecular liquids<sup>12,17</sup>.

When interactions between particles in a simple liquid are augmented by strong, short-ranged attractions, spatially averaged dynamical quantities change in non-trivial ways<sup>18,19,20,21</sup>. This situation has been realized experimentally by adding linear chain molecules to suspensions of colloidal particles, whose direct interactions are almost purely repulsive<sup>22</sup>. By varying  $\phi_p$  one can tune the fluid from purely repulsive to strongly attractive. For large colloid volume fraction,  $\phi_c$ , and vanishing attraction strength ( $\phi_p = 0$ ), the suspension is in essence a dense hard-sphere fluid with the basic phenomenology of simple supercooled liquids. As  $\phi_p$  increases, however, relaxation accelerates significantly, so that a hard-sphere glass can be “melted” by adding attractions<sup>18</sup>. Beyond a certain value of  $\phi_p$ , relaxation becomes instead more sluggish as more polymer is added, leading to re-vitrification

at large  $\phi_p$ .

In this Letter we examine whether the peculiar behavior of attractive colloids reflects fundamental changes in the nature of dynamical heterogeneity. Although extensive computational work has been done to characterize such heterogeneity in simple liquids, previous simulations of materials with short-ranged attractions have not focused on correlated microscopic motions. For this purpose we have adopted the model of Puertas *et al.* for polymer-mediated interactions between colloids<sup>19,20</sup>. The effective interaction potential between a pair of colloids separated by distance  $r$ , described in detail in Refs. 21-22, is plotted in Fig. 1 for the values of  $\phi_p$  we have studied. Interactions consist of a short-ranged repulsion parameterized by the sum of particle radii, a short-ranged attraction that mimics the polymer-induced depletion interaction, and a slowly varying, long-ranged repulsion designed to prohibit phase separation<sup>23</sup>. The effective range and form of each term are precisely as given in Refs. 21-22. We have focused on weakly polydisperse systems, in which these radii are drawn from a flat distribution with mean  $a$  and half-width  $\delta a = a/10$ . In this Letter all quantities with units of length have been scaled by the mean radius  $a$ , and quantities with units of time have been scaled by  $t_0 = \sqrt{\frac{8a^2}{9v^2}}$ , with  $v$  the thermal velocity, which is set to  $v^2 = \frac{8}{9}$ . We have used standard methods of molecular dynamics to propagate equilibrated systems of 1000 periodically replicated colloidal particles, stochastically rescaling colloid momenta every 101 time steps to maintain a Boltzmann distribution at temperature  $T = \frac{3}{2}v^2 = \frac{4}{3}$ . We have investigated a single colloid volume fraction  $\phi_c = \frac{4\pi N}{3V}a^3(1 + (\delta a/a)^2) = 0.55$  and several polymer volume fractions (i.e., attraction strengths as plotted in Fig. 1) ranging from  $\phi_p = 0.05$  to  $\phi_p = 0.375$ .

In order to contrast features of dynamic heterogeneity unique to attractive systems with those generic to simple supercooled liquids, we have selected a colloid density for which relaxation is already very slow for  $\phi_p = 0$ . The self-diffusion constant  $D(\phi_p)$ , plotted in Fig. 1 as a function of  $\phi_p$ , thus evinces the re-entrant behavior we have described. Specifically,  $D$  decreases by two orders of magnitude as  $\phi_p$  approaches 0.25 and then increase sharply for higher polymer concentrations.

The non-Gaussian parameter, plotted in Fig. 1(b) as a function of time for several values of  $\phi_p$ , indicates that short-ranged attractions effect changes more profound than simply a renormalized average time or length scale<sup>19,20</sup>. The peak of  $\alpha_2(t)$  roughly locates the time of maximum dynamic heterogeneity. We denote the time corresponding to this peak as  $t^*$ . The dependence of  $t^*$  on  $\phi_p$  closely mirrors that of the diffusion constant, reflecting a global change in relaxation time. But the shape and scale of  $\alpha_2(t)$  also change significantly with attraction strength. Most notably, the peak height  $\alpha_2(t^*)$  declines by nearly an order of magnitude as  $\phi_p$  approaches 0.25, then grows rapidly for larger values of  $\phi_p$ . This

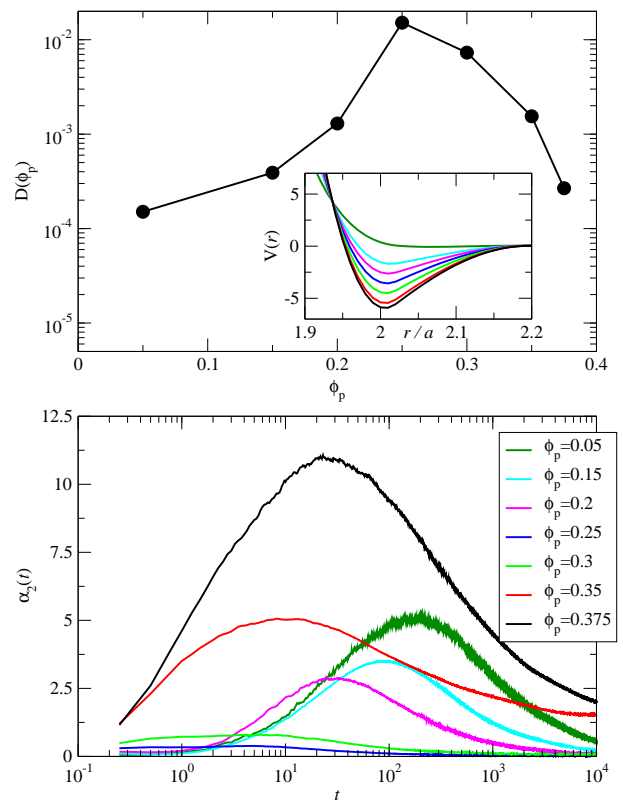


FIG. 1: (a) Diffusion constant  $D$  as a function of polymer volume fraction  $\phi_p$ . In each case,  $D$  was computed from the mean squared displacement averaged over particle size. Inset: Potential energy of interaction  $V(r)$  as a function of the distance  $r$  between two particles with radius  $a$  for the values of  $\phi_p$  we have studied numerically. From the least negative minimum of  $V(r)$  to the most negative minimum, these values are  $\phi_p = 0.05, 0.15, 0.2, 0.25, 0.3, 0.35$ , and  $0.375$ . (b) Non-Gaussian parameter  $\alpha_2(t)$  as a function of time  $t$ .

evolution strongly suggests a change in the character of microscopic dynamics<sup>19</sup>.

The full distribution of particle displacements provides a more detailed picture of microscopic rearrangements<sup>24</sup>. Fig. 2 shows a plot of  $\tilde{P}[\log_{10}(|\delta \mathbf{r}|), \tau_0]$  for states representative of weak attractions ( $\phi_p = 0.05$ ), strong attractions ( $\phi_p = 0.375$ ), and intermediate attraction strength ( $\phi_p = 0.25$ ). Since relaxation rates vary greatly among these three states, we have followed Cates *et al.* in comparing motion over time intervals  $\tau(\phi_p)$  yielding the same mean squared displacement,  $10a^2$ .<sup>24</sup> As reflected by  $\alpha_2(t)$ , the distributions at  $\phi_p = 0.05$  and  $\phi_p = 0.375$  are highly non-Gaussian, exhibiting distinct populations of especially mobile and especially immobile particles. Cates *et al.* have reported a similarly bimodal distribution of  $\log(|\delta \mathbf{r}|^2)$  for strongly attractive colloids at much lower densities ( $\phi_c = 0.4$ )<sup>24</sup>. Contrary to what is suggested in their work, however, we see that bimodality is by no means unique to strongly attractive systems. The distinction between mobile and immobile populations is

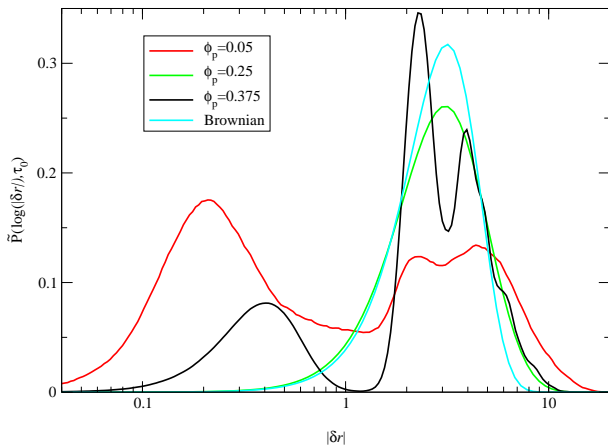


FIG. 2: Distributions  $\tilde{P}[\log_{10}|\delta\mathbf{r}|, \tau_0]$  of the logarithm of particle displacements  $|\delta\mathbf{r}|$  at time  $\tau_0$ . Results are shown for polymer volume fractions  $\phi_p = 0.05, 0.375$ , and  $0.25$ , and for a Gaussian distribution of  $\delta\mathbf{r}$ . Times  $\tau_0(\phi)$  and the width of the reference distribution were chosen to obtain a consistent mean squared displacement,  $\langle|\delta\mathbf{r}|^2\rangle = 10a^2$ .

in fact *more* pronounced when attractions are almost negligibly weak. This feature of dynamic heterogeneity is therefore common to sluggish systems with both weak and strong attractions. These two glassy states also share a degree of structure in  $\tilde{P}[\log_{10}(|\delta\mathbf{r}|), \tau_0]$  within the subpopulation of mobile particles. For  $\phi_p = 0.05$  particles clearly tend to move in discrete steps of approximately integer multiples of a typical particle diameter,  $2a$ . This feature highlights the decoupling of diffusion and structural relaxation in jammed liquids. Although fluctuations in local environment may permit a particle to move out of its cage, density correlations persist such that the newly formed cage has a well-defined spatial relationship with the original. Stepwise motion is much less pronounced at high  $\phi_p$ .

By contrast, the shape of  $\tilde{P}[\log_{10}|\delta\mathbf{r}|, \tau_0]$  at  $\phi_p = 0.25$  is nearly that of a Gaussian, plotted for reference in Fig. 2. There is evidence neither of a distinct population of immobile particles nor of stepwise motion. The statistics of single-particle displacements at intermediate attraction strength thus more strongly resemble those of a dynamically homogeneous fluid at lower density than those of a non-attractive fluid at the same density. The simplest conclusion is that the  $\phi_p = 0.25$  system is in essence dynamically uniform. Evidence exists, however, that correlated motions of neighboring particles do show signs of dynamic heterogeneity<sup>25</sup>. This situation could be expected if particle displacements were dominated by movement of clusters transiently stabilized by attractions<sup>25</sup>. Heterogeneity associated with formation and decay of a cluster would not have a strong signature in  $\tilde{P}[\log_{10}|\delta\mathbf{r}|, \tau_0]$  due to translation of the cluster as a whole.

The essence of a dynamic heterogeneity perspective

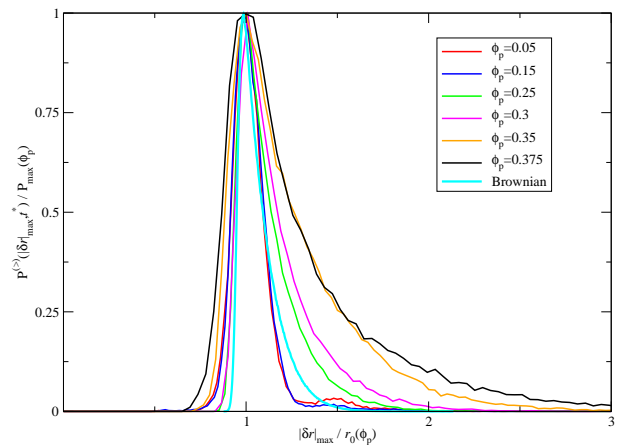


FIG. 3: Distributions  $P^{(>)}(|\delta\mathbf{r}|_{\max}, t^*)$  of maximum displacements for the 5% most mobile particles. We use as a measure of mobility  $|\delta\mathbf{r}|_{\max}$ , the *largest* displacement a particle undergoes (from its position at time  $t$ ) during the time interval  $t$  to  $t + t^*$ . Distributions and displacements have been scaled to coincide at the most likely value of  $|\delta\mathbf{r}|_{\max}$ . A scaled extreme displacement distribution is also plotted for a perfectly Brownian system of 1000 particles.

on glassy liquids is that relaxation over any short interval is driven by a small subset of particles that are temporarily much more mobile than the average. The statistics of extreme displacements should therefore be revealing of basic relaxation mechanisms<sup>10</sup>. Here we focus on particles among the 5% most mobile over an interval of length  $t^* \ll \tau$ . Distributions of maximum displacement magnitudes for these especially mobile particles,  $P^{(>)}(|\delta\mathbf{r}|_{\max}, t^*)$ , are plotted in Fig. 3 for each of the polymer volume fractions we have studied. For purposes of comparison, we have scaled  $|\delta\mathbf{r}|_{\max}$  by its most likely value for each  $\phi_p$ . We have included for reference the extreme value distribution that would be obtained for a Brownian analogue of our system<sup>26</sup>.

These scaled distributions reveal a monotonic trend toward broadly distributed mobile particle displacements as attraction strength increases. For weak attractions, the large-displacement tail of  $P^{(>)}(|\delta\mathbf{r}|_{\max}, t^*)$  is attenuated relative to a simple Brownian fluid. For strong attractions, this tail is greatly enhanced. Although the overall shape of the full displacement distribution for intermediate attraction strength is roughly Gaussian, statistics of the extreme subensemble demonstrate that mobile particles nonetheless execute larger jumps (relative to the average) than in a Brownian reference system. This fact is already apparent in the tail of  $\tilde{P}(\delta\mathbf{r}, \tau)$  plotted in Fig. 2(b).

Individual particle trajectories provide a direct microscopic perspective on dynamic heterogeneity. The routes traced by several of the most mobile particles over a time  $t^*$  are plotted in Fig. 4 for the smallest and largest values of  $\phi_p$ . The dynamical features we have gleaned from

probability distributions are reinforced by these images. For the case of weak attractions in panel (a), the discrete nature of particle motion and correlations between subsequent cages are immediately evident. Even the most mobile particles spend the majority of this time interval confined to two or more regions of size  $\sim 2a$ . Trajectories are qualitatively different for the case of strong attractions in panel (b). Here, caged particles explore much smaller regions, while mobile particles explore much more diffuse regions. Regions of facile particle motion are clustered in space and markedly elongated, with asymmetries apparently correlated over several particle radii.

Most of the qualitative changes in dynamical heterogeneity we have reported can be understood as consequences of changing spatial patterns of structural defects. Models based on dynamical heterogeneity typically assume that the subtle defects which enable local relaxation are sufficiently sparse as to be statistically independent. We have proposed that an important effect of short-ranged attractions is to introduce non-negligible spatial correlations among such facilitating entities<sup>27</sup>. In particular, defects should aggregate with increasing attraction strength as an indirect result of particle clustering. Microscopic regions of mobility thus grow in size while becoming still more sparse. This picture accounts for the broadening distributions of mobile particles we have computed. Particle trajectories depicted in Fig. 4 make the agreement especially vivid. The limited size of facilitating defects in a hard sphere glass cuts off the range of available displacements. Clustering of these defects as attractions are introduced provides increasingly extended loose regions for mobile particles to explore. We believe our numerical results provide strong evidence for segregation of jammed and unjammed regions of attractive liquids, even at such large values of  $\phi_c$ .

In summary, the change in dynamics induced by short-ranged attractions in a dense model liquid is dramatic even on the microscopic scale. Our results reveal three distinct regimes of dynamical heterogeneity. For weak attractions, mobilized particles make discrete jumps between cage structures, which may remain correlated over many jump times. For a range of intermediate attraction strengths, Gaussian particle displacement statistics suggest instead very fluid and uniform motion. The role of attractions in this regime, we suggest, is to bind small transient clusters which move on a time scale comparable to their lifetimes. Strong attractions restore some discreteness of particle displacements, presumably because transient clusters are too large to move appreciably on pertinent time scales. We thus conclude that “attractive” glassiness is driven by enhanced sparseness of mobilizing defects, which behave as if attracted to one another. We

are pursuing further calculations to confirm this clustering of mobility in dense environments and to characterize the correlated fluctuations underlying fluidity at intermediate attraction strength.

We would like to thank Laura Kaufman for useful discussions. We acknowledge the NSF (D.R.R.), DOE

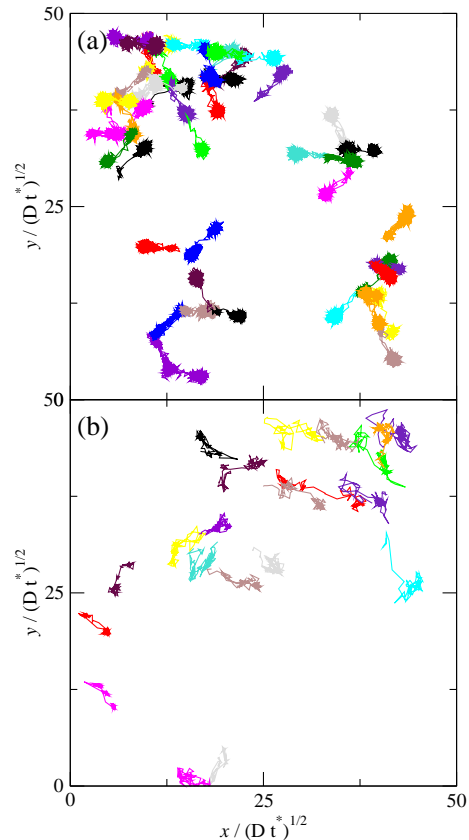


FIG. 4: Representative trajectories of length  $t^*$  for several particles exhibiting large displacements in the  $xy$ -plane. Trajectories have been projected onto this plane for graphical simplicity. Systems with  $\phi_p = 0.05$  and  $\phi_p = 0.375$  are depicted in panels (a) and (b), respectively.  $x$  and  $y$  axes have been scaled by the length  $\sqrt{Dt^*}$  characterizing diffusive motion.

(P.L.G.), and the United States-Israel Binational Science Foundation (D.R.R. and E.R.) for financial support. D.R.R. is a Camille Dreyfus Teacher-Scholar and an Alfred P. Sloan Foundation Fellow.

<sup>1</sup> U. Balucani and M. Zoppi, *Dynamics of the Liquid State* (Oxford, New York, 1994).

<sup>2</sup> W. Kob *et al.*, Phys. Rev. Lett. **79**, 2827 (1997).

<sup>3</sup> C. Donati *et al.*, Phys. Rev. Lett. **80**, 2338 (1998).

- <sup>4</sup> D. N. Perera and P. Harrowell, Phys. Rev. E **54**, 1652 (1996).
- <sup>5</sup> R. Yamamoto and A. Onuki, Phys. Rev. E **58**, 3515 (1998).
- <sup>6</sup> L. A. Deschenes and D. A. Vanden Bout, Science **292**, 255 (2001).
- <sup>7</sup> E. V. Russell and N. E. Israeloff, Nature **408**, 695 (2000).
- <sup>8</sup> S. A. Reinsberg *et al.*, J. Chem. Phys. **114**, 7299 (2001).
- <sup>9</sup> E. R. Weeks *et al.*, Science **287**, 627 (2000).
- <sup>10</sup> C. Donati *et al.*, Phys. Rev. E **60**, 3107 (1999).
- <sup>11</sup> S. Butler and P. Harrowell, J. Chem. Phys. **95**, 4454 (1991).
- <sup>12</sup> J. P. Garrahan and D. Chandler, Proc. Nat. Acad. Sci. **100**, 9710 (2003).
- <sup>13</sup> J. P. Garrahan and D. Chandler, Phys. Rev. Lett. **89**, 035704 (2002).
- <sup>14</sup> S. Whitelam, L. Berthier, and J. P. Garrahan, Phys. Rev. Lett. **92**, 185705 (2002).
- <sup>15</sup> S. Whitelam and J. P. Garrahan, Facilitated spin models in one dimension: a real-space renormalization group study, cond-mat/0405647.
- <sup>16</sup> M. Vogel and S. C. Glotzer, Temperature dependence of spatially heterogeneous dynamics in a model of viscous silica, cond-mat/0404733.
- <sup>17</sup> L. Berthier and J. P. Garrahan (unpublished).
- <sup>18</sup> K. Dawson *et al.*, Phys. Rev. E **63**, 011401 (2001).
- <sup>19</sup> A. M. Puertas, M. Fuchs, and M. E. Cates, Phys. Rev. Lett. **88**, 098301 (2002).
- <sup>20</sup> A. M. Puertas, M. Fuchs, and M. E. Cates, Phys. Rev. E **67**, 031406 (2003).
- <sup>21</sup> L. Fabbian *et al.*, Phys. Rev. E **59**, R1347 (1999).
- <sup>22</sup> K. N. Pham *et al.*, Science **296**, 104 (2002).
- <sup>23</sup> The effect of such a term on the type of heterogeneous motion discussed here has not been unambiguously demonstrated. Nor is it clear that such a repulsion exists between colloidal particles studied in experiments.
- <sup>24</sup> M. E. Cates *et al.*, Theory and simulation of gelation, arrest and yielding in attracting colloids, cond-mat/0403684.
- <sup>25</sup> D. R. Reichman, E. Rabani, and P. L. Geissler (unpublished).
- <sup>26</sup> E. J. Gumbel, *Statistics of Extremes* (Columbia University Press, New York, 1958).
- <sup>27</sup> P. L. Geissler and D. R. Reichman, Short-ranged attractions in jammed liquids: How cooling can melt a glass, cond-mat/0402673.